Microstructure and mechanical properties of fine-grained thin-walled AZ91 tubes processed by a novel combined SPD process

H ABDOLVAND[1], G FARAJI[1],*, J SHAHBAZI KARAMI[2] and M BANIASADI[1]

[1]School of Mechanical Engineering, College of Engineering, University of Tehran, Tehran 11155-4563, Iran
[2]Faculty of Mechanical Engineering, Shahid Rajaee Teacher Training University, Tehran 16788-15811, Iran
*Author for correspondence (ghfaraji@ut.ac.ir)

Abstract. A combination of parallel tubular channel angular pressing (PTCAP) and tube backward extrusion (TBE) as a novel combined severe plastic deformation (SPD) was applied on AZ91 alloy to produce ultrafine-grained (UFG) thin-walled tubes. The effects of combined SPD process were investigated on the microstructure refinement and mechanical properties. Also, hydro-bulge test was carried out to reveal the mechanical properties. The results showed a notable increase in ultimate strength, yield strength and microhardness of the thin-walled UFG tube were achieved compared to that from PTCAP process. A remarkable grain refinement achieved. Applying three-passes-combined process refine the grain size to 8.8 μm from an initial value of ∼150 μm. For one pass- and two passes-processed thin-walled tubes, it was about 12.4 and 9.8 μm, respectively. Yield and ultimate strengths were increased notably to 150 and 354 MPa for 2P+TBE tube, from the initial values of 86 and 166 MPa, respectively. The maximum microhardness was increased to about 105 Hv for the 2P+TBE tube from the initial value of 56 Hv. Hydro-bulge test showed that the bursting pressure increased to 246 bar for 2 passes-thin-walled tube from the initial value of 160 bar. It was 220 and 195 bar for 1 pass- and 3 passes-thin-walled tubes, respectively.

Keywords. Severe plastic deformation; thin-walled tube; ultrafine-grained; AZ91; hydro-bulge test.

1. Introduction

In recent years, numerous researchers have focussed on proposing severe plastic deformation (SPD) methods due to the superior mechanical and physical properties of ultrafine-grained (UFG) materials [1,2]. In all SPD methods, a significant plastic strain is imposed without any substantial cross-sectional change of the workpiece to generate UFG and nanograined (NG) materials [3]. Among the introduced SPD process, high-pressure torsion (HPT) [4,5], equal channel angular pressing (ECAP) [6–9], accumulative roll bonding (ARB) [10,11] and cyclic extrusion compression (CEC) [12], are the most successful techniques for industrial applications. Although there is a need to use high strength and especially, high strength to weight ratio tubes in a broad range of industrial applications, namely aerospace, petroleum industries and others, most of the introduced SPD methods were developed for sheet- and bulk-shaped materials and only a few processes have been proposed for tubular materials. High-pressure tube twisting (HPTT) [13], accumulative spin bonding (ASB) [14] and tube cyclic extrusion compression (TCEC) [15] were proposed as efficient SPD techniques for tubular materials. Also, Faraji *et al* [16–19] have developed two novel effective methods of tubular channel angular pressing (TCAP) [16,17] and parallel tubular channel angular pressing (PTCAP) [18,19].

The PTCAP process gives better strain and hardness homogeneity, and it needs lower load force compared to TCAP methods [18]. As it is clear, hardness homogeneity and process load are two main challenges in SPD processing of metals. So, PTCAP is an privileged SPD method for producing UFG tubular samples.

Despite many applications of high strength thin-walled tubes, the developed SPD methods for the tubular material are not able to produce UFG thin-walled tubes, due to the effect of the friction force. As the thickness of the tube is reduced, the friction force to process load ratio remarkably increased. Recently, a successfully combined SPD process was proposed to solve the mentioned issue by the authors [20]. In that study, a commercial AZ31 alloy with just a single cycle of the combined process was performed. A significant grain refinement with completely homogenous microstructure even after a single cycle was achieved. The principle of the combined SPD process shown schematically in figure 1. As shown, this technique consists of two stages. First, PTCAP, and then TBE process are applied to the tube material for producing thin-walled UFG tube. The tube is pressed into the gap between the die and the mandrel during the PTCAP process. It comprises two half cycles, and during the process, the tube passes two shear zones in each half cycle. The diameter of the tube increased to a maximum value in the first half cycle and it
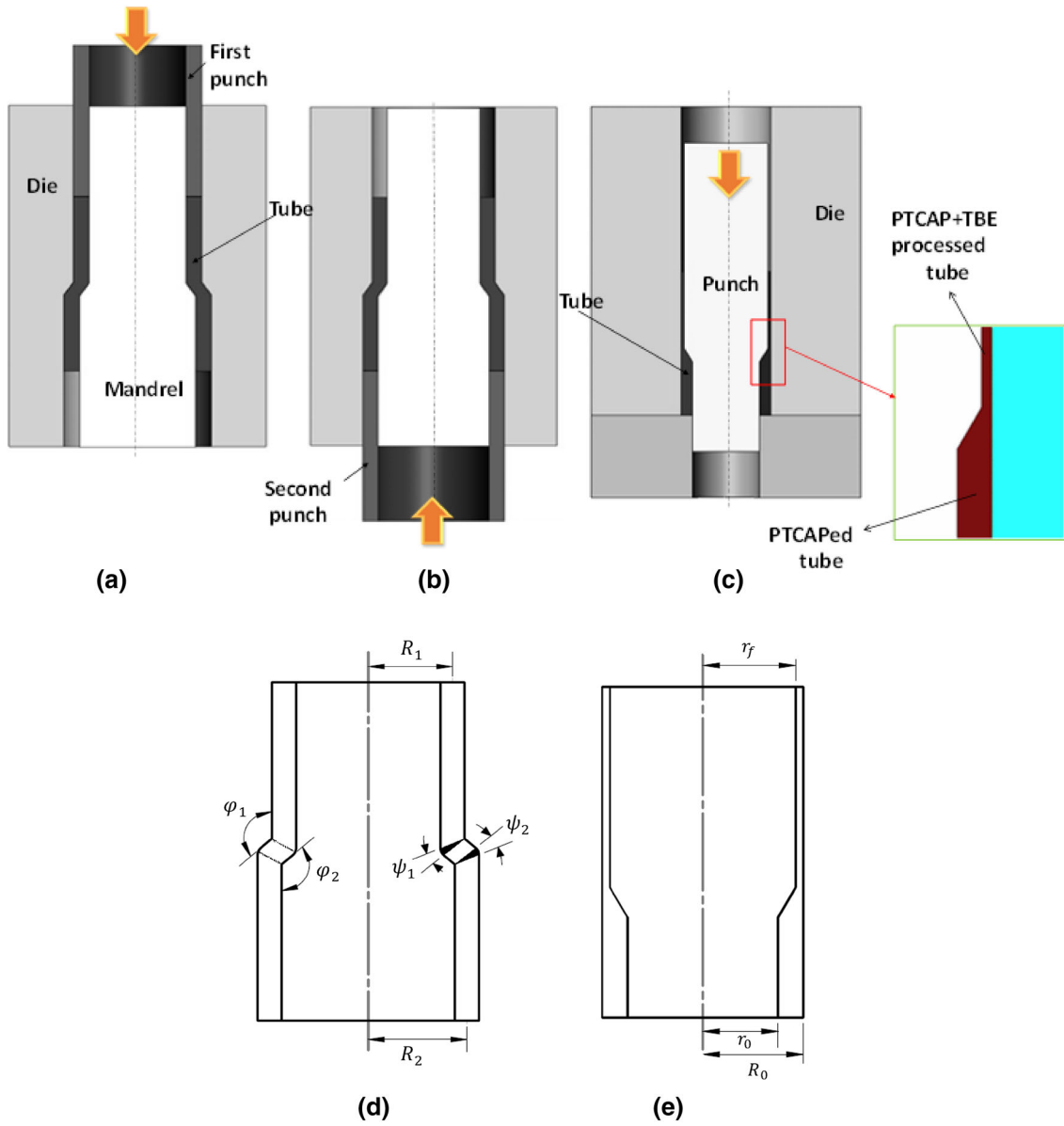
Figure 1. The combined process schematic; (**a**) the first and (**b**) the second half cycles of (**c**) PTCAP and TBE and die parameters of (**d**) PTCAP and (**e**) TBE stages.

decreased to an initial value in the second half cycle. After performing the considerable number of passes of the PTCAP process, the TBE process is done to reduce the thickness of the UFG tube. During the TBE process, the punch moves down and presses the tube to generate thin-walled tube. The total equivalent strain achieved from N cycles of the PTCAP process and TBE process can be obtained from the following equation [20]:

$$\bar{\varepsilon}_{\text{tot}} = 2N \left\{ \sum_{i=1}^{2} \left[\frac{2 \cot\left(\varphi_i/2 + \psi_i/2\right) + \psi_i \cosec(\varphi_i/2 + \psi_i/2)}{\sqrt{3}} \right] + \frac{2}{\sqrt{3}} \ln \frac{R_2}{R_1} \right\} + \ln \frac{R_0^2 - r_0^2}{R_0^2 - r_f^2} \tag{1}$$
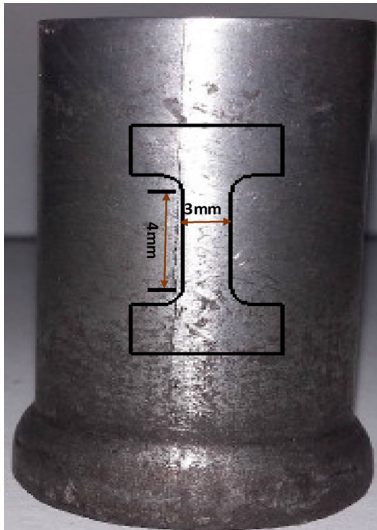
Figure 2. Tensile test dimension on PTCAP processed tube.

In the current study, the novel combined SPD process was applied to a commercial AZ91 magnesium alloy for the first time. The AZ91 alloy tubes were treated with PTCAP up to three cycles followed by TBE to demonstrate the effect of the number of passes on the mechanical properties, microstructural evolution and microhardness variations of thin-walled UFG tubes.

Also, a hydro-bulge test was performed on the thin-walled tubes to evaluate the effect of the grain size on bursting pressure of UFG tubes. Because the stress-state in the hydro-bulge test can reveal the properties of tubes better [21]. A formula was proposed to predict the bursting pressure of thin-walled tubes as follows [22]:

$$P_{\mathrm{b}} = \overline{\sigma}_{\mathrm{u}} \left(\frac{0.25}{\overline{\varepsilon}_{\mathrm{u}} + 0.227} \right) \left(\frac{2.718}{\overline{\varepsilon}_{\mathrm{u}}} \right)^{\overline{\varepsilon}_{\mathrm{u}}} \left(\frac{2t}{d} \right), \qquad (2)$$

where $P_{\mathrm{b}}, \overline{\sigma}_{\mathrm{u}}, \overline{\varepsilon}_{\mathrm{u}}, t$ and d are bursting pressure, equivalent ultimate stress, equivalent ultimate strain, mean diameter and thickness of the tube, respectively.

2. Experimental

AZ91 magnesium alloy was used as an experimental material which processed by the combined SPD process. Tube-shaped samples with outer diameter of 20 mm, thickness of 2.5 mm and length of 40 mm were prepared. PTCAP and TBE processes die parameters are shown in figure 1, in which the channel angle $\varphi_1 = \varphi_2 = 120°$, the curvature angle $\psi_1 = \psi_2 = 0°$ and $r_{\mathrm{f}} = 75$ mm. By application of these parameters, equivalent strains of about 1.6 and 1.2 are applied to the tube after each cycle of PTCAP and TBE processes, respectively. The PTCAP process was implemented to the
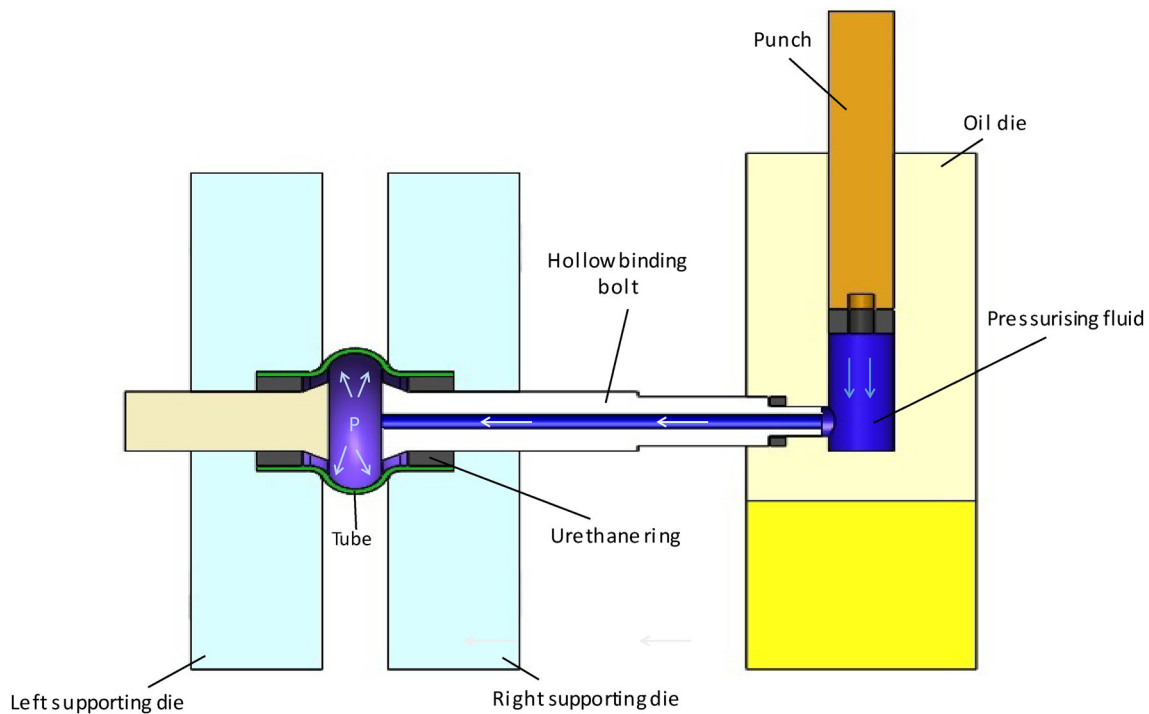

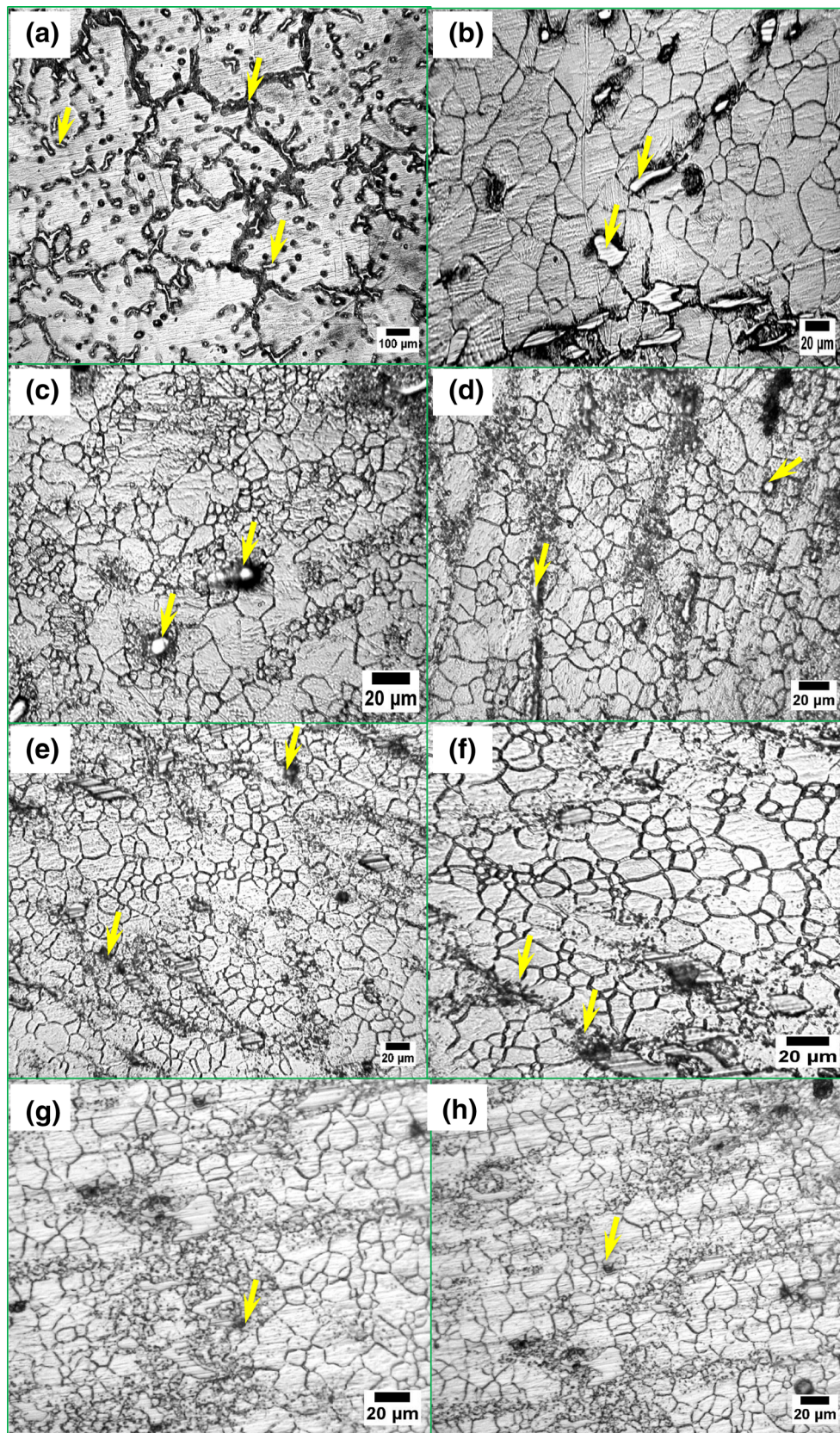**Figure 3.** Schematic illustration of the tool setup for the hydro-bulge test.

Figure 4. Optical micrographs of AZ91 alloys: (**a**) 0P, (**b**) 0P+TBE, (**c**) 1P, (**d**) 1P+TBE, (**e**) 2P, (**f**) 2P+TBE, (**g**) 3P and (**h**) 3P+TBE processed tubes.
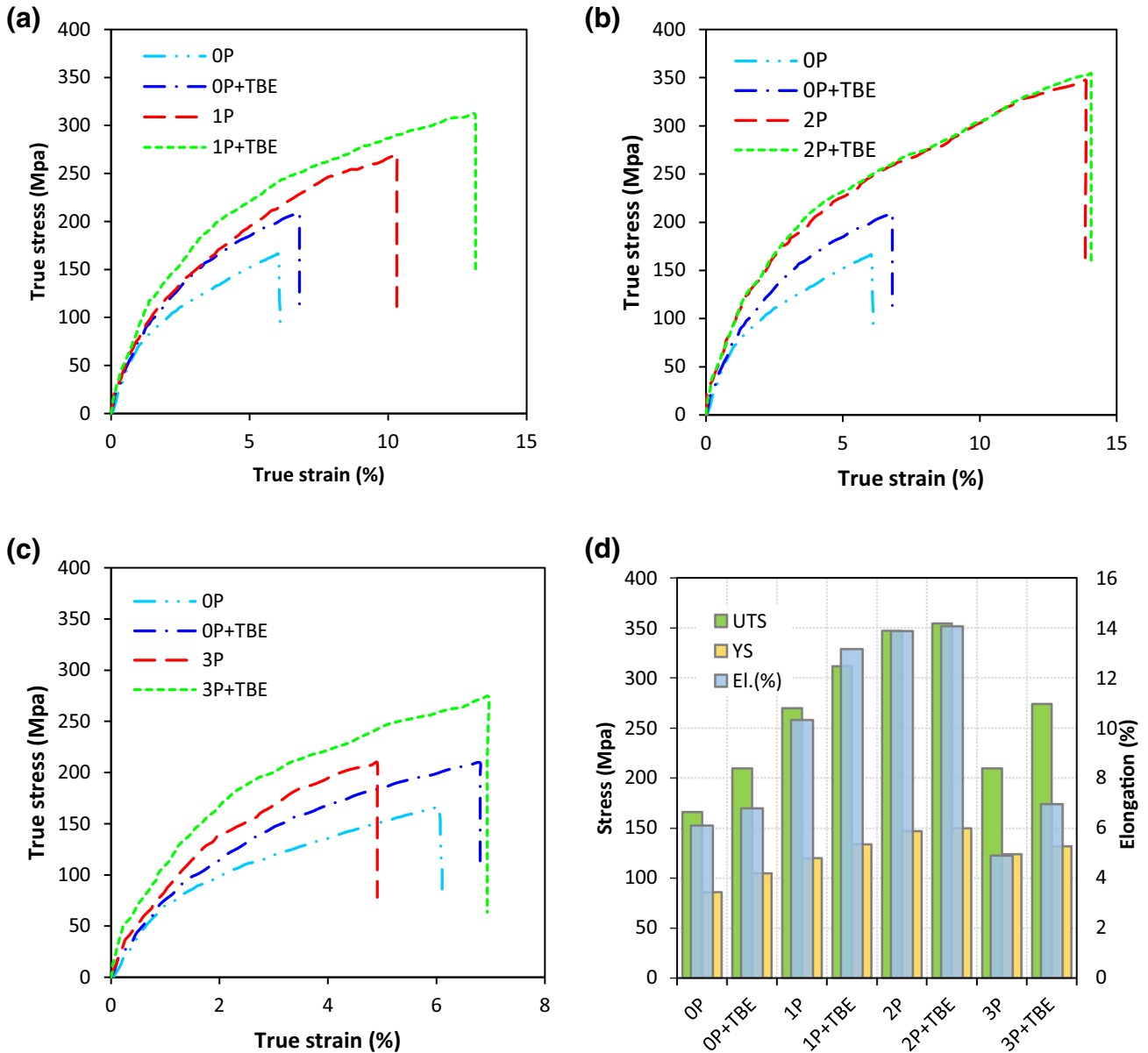
Figure 5. True stress *vs.* true strain curves for 0P and 0P+TBE samples with (**a**) 1P and 1P+TBE, (**b**) 2P and 2P+TBE and (**c**) 3P and 3P+TBE samples. (**d**) UTS, YS and elongation of different specimens.

tubes through one, two and three passes, then the TBE process reduce the thickness of the tubes remarkably from 2.5 to 0.75 mm. All the die set components were manufactured from hot-worked tool steel and hardened to 55 HRC. The following notations are used as the names of the samples in the text. '0P', '1P', '2P' and '3P' stand for as-cast, 1 pass, 2 passes and 3 passes PTCAP processed tubes, respectively. Also, '0P+TBE', '1P+TBE', '2P+TBE' and '3P+TBE' stands for as-cast+TBE, 1 Pass PTCAP+TBE, 2 Passes PTCAP+TBE, 3 Passes PTCAP+TBE thin-walled tubes, respectively.

The combined SPD process was performed at the ram speed of 10 mm min^{-1} at a temperature of 573 K (300°C), while using molybdenum disulfide (MoS$_2$) as a lubricant. Tensile

test samples were prepared from the axial direction of the processed tube as shown in figure 2 and carried out with the initial strain rate of 0.001 s^{-1} at room temperature. To investigate the microstructure evolution, optical microscopy (OM) was used. A linear intercept method, was used to measure the grain sizes of the processed samples. The surfaces of the processed tubes were prepared by the standard metallographic methods. The Vicker's microhardness testing was done with a load of 100 g, which was applied for 15 s.

To study the variations of bursting pressure of the processed thin-walled tubes, the hydro-bulge test was implemented. The die setup is shown schematically in figure 3. Avoiding the use of expensive hydraulic equipment and easily supplying of the

high-pressure fluid are the main advantages of this tooling. As illustrated, the fluid is pressurized by moving down the punch. The rising of the fluid pressure continues until the tube bursts. The hydro-bulge test was conducted by a 300KN Universal INSTRON press at a punch speed of 2 mm min^{-1}. To analyse the fracture surfaces of the burst tubes and tensile test samples, the scanning electron microscope (SEM) was utilized.

3. Results and discussion

3.1 *Microstructure evolution*

The optical micrographs of AZ91 alloys and their histograms of grain distribution are shown in figures 4 and 5, respectively. Figure 4a demonstrates the microstructure of unprocessed material containing coarse grains with a mean grain size of ~150 μm. As depicted, there is a dendritic structure with networks of β phase (Mg$_{17}$Al$_{12}$) at α-Mg grain boundaries [17,23–25]. It was shown by arrows in figure 4. The formation of β phase network is clearly harmful to mechanical properties, especially ductility. After performing the TBE process of the as-cast tube, dynamic recrystallization occurred, and equiaxed grain was formed (figure 4b). The activation of slip system in magnesium alloys considerably depends on the deformation temperature. Therefore, the combined SPD process was performed at 573 K (300°C). Because of the lack of slip systems in HCP metals, many twins occurred in the original grain. A severe normal strain and dynamic recrystallization give a homogeneous structure. The previous studies showed that dynamic recrystallization could occur during deformation of AZ91 at 573 K (300°C) [26]. As it can be seen, β phase is broken to relatively smaller particles and distributed in the microstructure [27]. A structure of fine, homogeneous and equiaxial β phase distributing inside α phase improves formability and mechanical properties of magnesium alloys [28]. The 0P+TBEed tube (figure 4b) shows almost homogeneous distribution, but the grain sizes are not fine enough, and the mean grain size decreased to 20.8 μm. A typical inhomogeneous microstructure of 1P tube is shown in figure 4c. However, the mean grain size decreased to 12.6 μm. As depicted, fine recrystallized grains appear along grain boundaries and through some coarse grains. However, small grains density is much lower in the large grain size area, and dynamic recrystallization was incomplete. The β phase is broken heavily and spread randomly along the α-Mg phase. The shear strains play the primary role in grain refinement. So, increasing the shear strain leads to replacing fine recrystallized grains [29]. The homogenous, fine and equiaxed grains obtained after the 1P+TBE process (figure 4d), such as previous research on AZ31 alloy [20]. Because of the high strain value, the β phase dissolution occurs more readily, and the mean grain size decreased to about 12.4 μm. By increasing the number of the passes of the PTCAP process, shear strain increased, and as a result, grain size decreased (figure 4e and

g). To reduce the thickness of the UFG 2P and 3P tubes, the TBE process was performed. Eventually, the TBE process could more refine and equiaxed grains and dissolve the β phase completely, as illustrated in figure 4f and h. The fine grains size was increased and existed in the microstructure. Finally, the mean grain size decreased to about 8.8 μm for 3P+TBE sample. The results of microstructure evolution are consistent with the previous studies by Galiyev *et al* [30] and Ding *et al* [31]. Consequently, it can be concluded that dynamic recrystallization occurs during hot deformation of AZ91 alloy. With increasing strain, the low angle grain boundaries grow to high angle grain boundaries, and β phase precipitates are crushed into small blocks and distributed at the newly formed dynamic recrystallized grain boundaries [32].

3.2 *Mechanical properties*

Figure 5 shows the tensile true stress–strain curves of the processed AZ91 alloy tubes after a different number of passes at
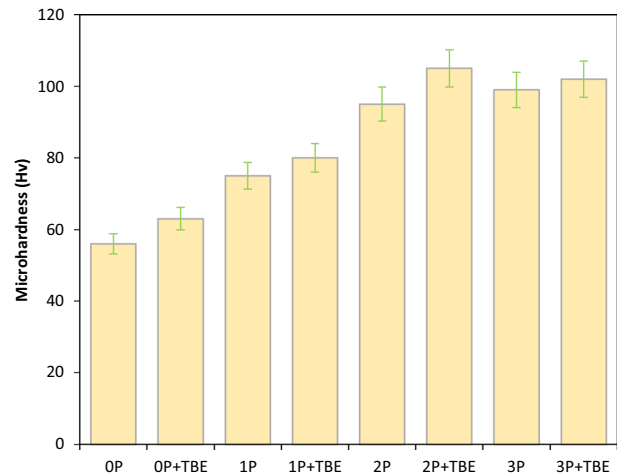

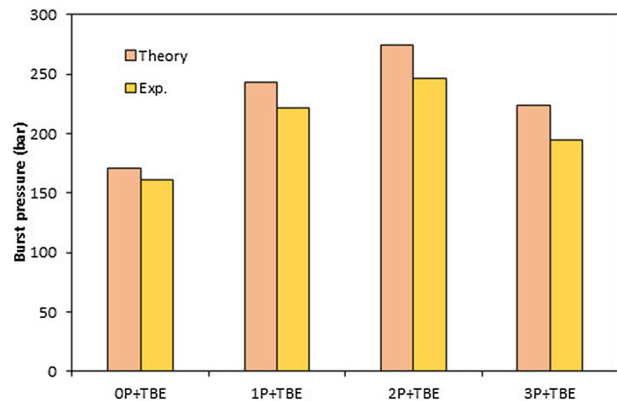**Figure 6.** Microhardness of the processed samples through different routes.

Figure 7. Bursting pressure of thin-walled tubes in the hydro-bulging test.
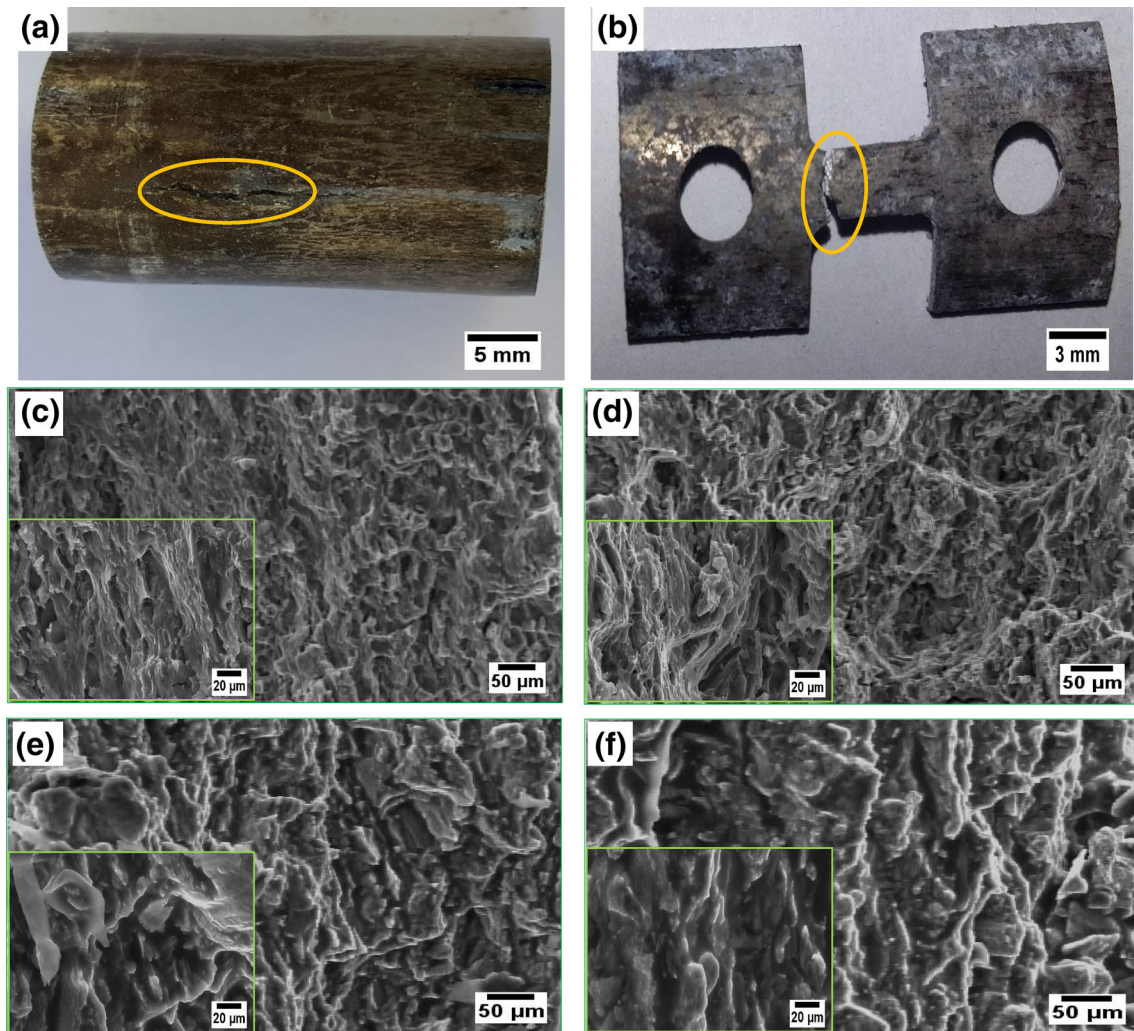
Figure 8. Fractured (**a**) hydro-bulge test and (**b**) tensile test sample of the 1P+TBE tube, SEM images showing fracture surfaces of (**c**) 0P+TBE, (**d**) 1P+TBE after tensile test and (**e**) 0P+TBE, (**f**) 1P+TBE processed samples after hydro-bulge test.

room temperature. It indicates that the combined SPD process increased the strength of the processed sample. Also, in all the processed tubes, the strength of the thin-walled tubes (TBEed samples) are more than the thick tubes (PTCAPed samples). Refining and homogeneous distribution of the recrystallized grains and increasing the dislocation density after the SPD process results in a remarkable increase in the strength [33]. The primary reason for the poor mechanical properties of the as-cast AZ91 is the inhomogeneous distribution of the β phase precipitates at the grain boundaries [23]. Jin *et al* [34] and Kim *et al* [35] studied the SPD process of AZ31 and AZ61 alloys, respectively. They reported that increasing the strain leads to increase in the elongation and decrease in strength as a result of texture evolution and grain refinement. In contrast, in the presently studied AZ91 alloys, both strength and elongation increased with increasing the strain. This difference between AZ91 alloy and other AZ series alloys could

be attributed to the higher volume fraction of β phase precipitates, and more homogeneous grain size distribution, which is responsible for increasing the elongation. For all the tubes, the strength of the PTCAP+TBEed tubes are higher compared to the PTCAPed tube because as discussed earlier, the grains of the PTCAP+TBEed tubes are more homogenous and refiner. Increase in the ultimate strength was continued significantly from 166 for the 0P sample to 354 MPa for 2P+TBE sample. The strength of the 3P tube decreased severely to 209 MPa, because of the existence of microcrack on the surface of the tube. However, after 3P+TBE process, the strength is increased again. It should be noted that the TBE process in addition to producing thin-walled UFG tubes could improve the mechanical properties of PTCAPed tubes.

The Vicker's microhardness variation of the processed tubes is demonstrated in figure 6. As obvious, a notable increase in microhardness was obtained just after 1P process.

The hardness was rised from 56 (0P sample) to 75 Hv (1P processed sample). The hardness of further processed specimens showed that increase in the hardness was continued to maximum 105 Hv for the 2P+TBE sample. The hardness enhancement is in good agreement with the microstructure of the samples. More plastic strain leads to more grain refinement, better β phase distribution and consequently more hardness values. The hardness of the β phase is significantly higher than α-Mg phase [36]. Therefore, the increase in hardness could be due to the increase in β phase fracture and better distribution when plastic deformation occurs. Also, it is accepted that hcp metals exhibit a strong grain size dependency of hardness and strength due to lack of slip system [37].

Figure 7 shows the variations of the bursting pressures in the thin-walled processed tubes. As it can be seen, the bursting pressures of all PTCAP+TBEed tubes are considerably higher than the 0P+TBEed tube, which is consistent with the result of the ultimate strength obtained from the tensile test. The bursting pressure of the as-cast+TBEed tube increased from about 160 to 220 bar just after the 1P+TBE process. The maximum bursting pressure was about 246 bar for the 2P+TBE tube. Also, the bursting pressures were calculated by the proposed formula to compare with the experimental data as depicted in figure 7. A small error of ∼6% was obtained for the 0P+TBE tube. However, after 1P+TBE, 2P+TBE and 3P+TBE processes, the error increased to 9, 10 and 13%, respectively. Increasing the error may be related to the severe anisotropy enhanced by the PTCAP process [38]. The hydro-bulge test was performed at room temperature, and there was poor bulge height on the thin-walled burst tubes. Huang *et al* [39] reported that the planar basal texture in magnesium alloys imposes strong influence on the tube formability, and it leads to exhibit poor bulge height.

Figure 8a and b shows the results of the tensile test and hydro-bulge test of the 1P+TBE tube (the fracture area are marked). As shown, samples exhibit brittle rupture and no tendency to neck. To compare and investigate the fractured surfaces of burst and tensile tested thin-walled tubes and also the effect of the grain refinement, SEM micrograph test was performed which is shown in figure 8c–f. Magnesium alloys usually tend to fail brittle by cleavage or quasi-cleavage fracture [40,41]. As it is evident from figure 8c, some small cleavage planes and tearing edges can be observed, indicating a characteristic of quasi-cleavage fracture. The rupture model of the 0P+TBE tube was mainly brittle, which is ascribed to a coarse grain size and inhomogeneous coarse β phase distribution in the microstructure. Figure 8d shows some small tiny dimples appeared on the fracture surface of the 1P+TBE tube. This rupture model occurred by the formation and coalescence of microvoid ahead of the crack. Refining the grain size, precipitate and uniform distribution of the β phase lead to change the rupture model and increase the formability. As it can be seen from figure 8e–f, the hydro-bulge test change the type of the fracture of the samples. The hydro-bulge test changed the stress state and applied a biaxial tension stress. As depicted, the number of tiny dimples increased, and the fractured surfaces are flattered compared to the tensile test specimen. It means that the formability of the tubes under the hydro-bulge test is more than tensile-tested tubes. It is in agreement with the previous investigation on brass UFG tubes by the present authors [42].

4. Conclusion

This work presents an experimental investigation of a combined SPD process consisting PTCAP and TBE processes to produce UFG thin-walled tube for AZ91 magnesium alloys for the first time. The results are concluded as follows:

- A remarkable grain refinement achieved. Applying three-passes-combined process refine the grain size to 8.8 μm from an initial value of ∼150 μm. For one-pass and two-passes processed thin-walled tubes, it was about 12.4 and 9.8 μm, respectively.
- Yield and ultimate strengths were increased notably to 150 and 354 MPa for 2P+TBE tube, from the initial values of 86 and 166 MPa, respectively.
- The maximum microhardness was increased to about 105 Hv for the 2P+TBE tube from the initial value of 56 Hv.
- Hydro-bulge test showed that the bursting pressure increased to 246 bar for 2-passes thin-walled tube from the initial value of 160 bar. It was 220 and 195 bar for 1-pass and 3-passes thin-walled tubes, respectively.
- Study of the fractured surfaces showed that the tubes under hydro-bulge test exhibited more formability than under tensile test.

References

[1] Valiev R Z, Islamgaliev R K and Alexandrov I V 2000 *Prog. Mater. Sci.* **45** 103
[2] Spigarelli S, Mehtedi M E, Regev M, Gariboldi E and Lecis N 2012 *J. Mater. Sci. Technol.* **28** 407
[3] Suryanarayana C 1994 *Bull. Mater. Sci.* **17** 307
[4] Zhilyaev A P and Langdon T G 2008 *Prog. Mater. Sci.* **53** 893
[5] Wetscher F, Pippan R, Sturm S, Kauffmann F, Scheu C and Dehm G 2006 *Metall. Mater. Trans. A* **37** 1963
[6] Valiev R Z and Langdon T G 2006 *Prog. Mater. Sci.* **51** 881
[7] Jafarlou D M, Zalnezhad E, Hamouda A S, Faraji G, Mardi N A B and Mohamed M A H 2015 *Metall. Mater. Trans. A* **46** 2172
[8] Sanosh K P, Balakrishnan A, Francis L and Kim T N 2010 *J. Mater. Sci. Technol.* **26** 904
[9] Haghighi R D 2015 *Bull. Mater. Sci.* **38** 1205
[10] Saito Y, Utsunomiya H, Tsuji N and Sakai T 1999 *Acta Mater.* **47** 579

[11] Hidalgo P, Cepeda-Jiménez C, Ruano O A and Carreño F 2010 *Metall. Mater. Trans. A* **41** 758

[12] Chen Y J, Wang Q D, Roven H J, Karlsen M, Yu Y D, Liu M P et al 2008 *J. Alloys Compd.* **462** 192

[13] Tóth L S, Arzaghi M, Fundenberger J J, Beausir B, Bouaziz O and Arruffat-Massion R 2009 *Scr. Mater.* **60** 175

[14] Mohebbi M S and Akbarzadeh A 2010 *Mater. Sci. Eng. A* **528** 180

[15] Babaei A, Mashhadi M M and Jafarzadeh H 2014 *Mater. Sci. Eng. A* **598** 1

[16] Faraji G, Mashhadi M M and Kim H S 2011 *Mater. Lett.* **65** 3009

[17] Faraji G, Yavari P, Aghdamifar S and Mashhadi M M 2014 *J. Mater. Sci. Technol.* **30** 134

[18] Faraji G, Babaei A, Mashhadi M M and Abrinia K 2012 *Mater. Lett.* **77** 82

[19] Faraji G, Roostae S, Nosrati A S, Kang J and Kim H 2015 *Metall. Mater. Trans. A* **46** 1805

[20] Abdolvand H, Sohrabi H, Faraji G and Yusof F 2015 *Mater. Lett.* **143** 167

[21] Atkinson M 1997 *Int. J. Mech. Sci.* **39** 761

[22] Xue L, Widera G and Sang Z 2008 *J. Press. Vessel Technol.* **130** 014502

[23] Faraji G and Asadi P 2011 *Mater. Sci. Eng. A* **528** 2431

[24] Faraji G, Mashhadi M and Kim H S 2011 *Mater. Sci. Eng. A* **528** 4312

[25] Jamali S, Faraji G and Abrinia K 2016 *Mater. Sci. Eng. A* **666** 176

[26] Faraji G and Kim H S 2017 *Mater. Sci. Technol.* **33** 905

[27] Reshadi F, Faraji G, Aghdamifar S, Yavari P and Mashhadi M 2015 *Mater. Sci. Technol.* **31** 1879

[28] Lin J, Wang Q, Peng L and Roven H J 2009 *J. Alloys Compd.* **476** 441

[29] Shin D H, Kim I, Kim J and Zhu Y T 2002 *Mater. Sci. Eng. A* **334** 239

[30] Galiyev A, Kaibyshev R and Gottstein G 2001 *Acta Mater.* **49** 1199

[31] Ding H, Liu L, Kamado S, Ding W and Kojima Y 2007 *Mater. Sci. Eng. A* **452–453** 503

[32] Xu S, Matsumoto N, Kamado S, Honma T and Kojima Y 2009 *Scr. Mater.* **61** 249

[33] Sakai T and Miura H 2011 *Mechanical properties of fine-grained magnesium alloys processed by severe plastic forging.* INTECH Open Access Publisher

[34] Jin L, Lin D, Mao D, Zeng X and Ding W 2005 *Mater. Lett.* **59** 2267

[35] Kim W J, Hong S I, Kim Y S, Min S H, Jeong H T and Lee J D 2003 *Acta Mater.* **51** 3293

[36] Yoo M S, Kim J J, Shin K S and Kim N J 2002 *Magnesium Technology 2002 as held at the 2002 TMS Annual Meeting*, p 95

[37] Chino Y, Kobata M, Iwasaki H and Mabuchi M 2003 *Acta Mater.* **51** 3309

[38] Tavakkoli V, Afrasiab M, Faraji G and Mashhadi M M 2015 *Mater. Sci. Eng. A* **625** 50

[39] Huang C, Huang J, Lin Y and Hwang Y 2004 *Mater. Trans.* **45** 3142

[40] Lü Y, Wang Q, Zeng X, Zhu Y and Ding W 2001 *Mater. Sci. Eng. A* **301** 255

[41] Yue T, Ha H and Musson N 1995 *J. Mater. Sci.* **30** 2277

[42] Abdolvand H, Faraji G, Givi M B, Hashemi R and Riazat M 2015 *Met. Mater. Int.* **21** 1068